Published by :
http://www.ijert.org

International Journal of Engineering Research & Technology (IJERT)
ISSN: 2278-0181
Vol. 10 Issue 01, January-2021

Effect of Copper Oxide on Biodegradable Polymer Nanocomposite Thin Films

G. T. Padma[1],
[1]Department of Physics,
Sri Krishnadevaraya University, Anantapuramu,
Andhra Pradesh- 515003, India.

Thota Subba Rao[1]
[1]Department of Physics,
Sri Krishnadevaraya University, Anantapuramu,
Andhra Pradesh- 515003, India.

Venkata Ramana Mudinepalli[1*]
[1]Department of Physics,
Sri Krishnadevaraya University, Anantapuramu,
Andhra Pradesh- 515003, India.

***Abstract* - Sodium Alginate doped with Copper oxide composite polymer films was developed through Solution casting method. The structural properties on these polymer nanocomposite thin films were characterized by X-ray diffraction. XRD shows all the individual constituents of these composites and the CuO peaks increases as CuO increased in the composites. Thermogravimetric analysis (TGA) technique was used for thermal stability of these composites. Temperature dependence of dielectric properties of these SA/CuO nanocopmosite polymer thin films we measured in the frequency range from 100 Hz to 5 MHz. Dielectric properties of these composites strongly depends on the percentage of CuO and structure of these matrix. These type of composites are attracted much attention in battery applications.**

Keywords* - *Sodium Alginate, X-ray diffractometer, Solution Casting Method, Polymer nanocomposites, Dielectric properties.

I. INTRODUCTION

Blending polymer products is the latest technique for optimizing different polymer matrices and is a valuable method for producing substances with an extensive diversity of characteristics. Polymer characteristics may be improved by combining two or more polymers and/or adding organic/inorganic components for use in various applications. The melt blending and solvent casting routes are the most common ways for the manufacturing of polymer blends or composites. The development of the dielectric polymer nanocomposite films based on organic polymer and inorganic metal oxides has attracted the attention of researchers due to its potential applications in electronic devices [1-3]. In the synthesis of the polymer nanocomposites, biopolymer has acquired great significance due to its novel properties. Sodium Alginate (SA) is one of the biodegradable polymers and it is an inexpensive better film-forming ability, and environmentally safe. In the last decade, extensive work has been carried out using SA membranes on the structural, morphological, thermal, mechanical, and optical properties [4-7]. SA doped with different metal oxides has been used in various applications such as energy storage devices [3], food industry [8], pervaporation [5], controlled drug delivery [9]. Nature of the electrical behavior like bonding of the grains, grain motion and conduction of the polymer nanocomposites was explained by the dielectric behavior. The dielectric properties of the materials not only depend on the polymer structure but also it is depending on the properties and the sizes of the particles used. Jundale et al., studied the structural and electrical properties of thin films of polyaniline doped with copper oxide which are fabricated on the glass substrate by spin coating method [10]. Siddiqui et al., reported the synthesis of CuO/Alginate composite with enriched electrical properties by the sol-gel method [11]. Shameem et al., observed high ionic conductivity with Sodium Lithium sulfide nanoparticles in the alginate matrix and was successfully fabricated by using microwave irradiation method [12]. Shital et al., investigated the electric modulus and dielectric relaxations in the PVA/ZnO composite films prepared by solution casting method [13]. Brijesh et al., reported the synthesis and electrical properties of metal nanoparticle and rare earth ion dispersed in polyvinyl alcohol film fabricated by the solvent evaporation method [14]. For the past few years, CuO has gained significant importance due to its monoclinic p-type semiconducting nature that possesses better electrical, catalytic and optical properties synthesized by simple reflux condensation method [15]. Besides, it has some promising applications in different fields such as gas sensors, electrochemical devices, light-emitting devices, solar cells, high-energy radiation, hydrogen storage systems, optical limiters, microwave observers, shielding materials, thermoelectric materials and lithium-ion batteries because of its environmental stability [15-18]. In this connection, we herein plan to synthesize the copper oxide nanoparticles by hydrothermal method and to incorporate them into the SA matrix to fabricate by ultrasonic-assisted solution casting method with varied concentrations of CuO to accomplish improved dielectric properties [19]. These type of composites are attracted much attention in battery applications.

II. EXPERIMENTAL METHODS

II.1. Synthesis of copper oxide nanoparticles

The stoichiometric ratio of $Cu(NO_3)_2 3H_2O$ and NaOH pellets were dissolved separately in distilled water with magnetic stirring. Then the prepared NaOH solution

International Journal of Engineering Research & Technology (IJERT)
ISSN: 2278-0181
Vol. 10 Issue 01, January-2021

was added drop by drop into the copper solution for half an hour under constant magnetic stirring. The precipitate color was changed from blue to black. Further, this colloidal suspension was transferred into the 200ml Teflon-lined autoclave. Then kept in a hot air oven at a temperature of 150°C for 8 hours. Later, this solution is centrifuged to get the powder sample. To remove strains and impurities from the obtained powders,it was with washed with distilled water and ethanol for several times. Then, the collected final product dried at a temperature of 80°C to get the required CuO nanoparticles.

II.2. Synthesis of SA-CuO polymer nanocomposite thin films

The required nanocomposite polymer films are prepared by a solution casting method [19, 20]. For this, 5gm of sodium alginate dissolved in the 90ml of distilled water under magnetic stirring. This stirring continues until the formation of the homogenous solution for 48 hours. Then the desired weight percent amount of CuO was dispersed in 10ml distilled water using a probe sonicator and the magnetic stirrer. This solution was poured into the SA solution through the process of stirring. Again, this solution was sonicated for 15min to achieve a good dispersion of CuO in the SA matrix. Later, this solution was poured into Petri dishes and left dry at room temperature. Then the films are peeled off and stored in the desiccator. The SA films have been fabricated with different concentrations i.e., 0%, 5%, 10%, 15% of the CuO. Thus, black colour freestanding films were obtained. These films named C0, C5, C10, and C15 respectively that are free of air bubbles.

II.3. Characterization techniques

X-ray diffraction profiles of the prepared polymer nanocomposites were recorded by using Bruker, X-Ray Powder Diffractometer, CuK_α, λ=0.15406nm. The Thermal Analysis System (TA Instruments, New Castle DE, UK) observed thermal stability of the SA-CuO polymer nanocomposite thin films. The degradation temperatures were evaluated by TA instruments (Model-STA, Q 600, USA). The morphology of the films was observed by using FE-SEM, ZEISS, Ultra-55 instrument. The dielectric properties were studied by using LCR HiTESTER (HIOKI 3532-50, Japan). These measurements are carried out in the temperature range of room temperature to 100°C and frequency ranging from 100 Hz – 5 MHz.

III. RESULTS AND DISCUSSION

III.1. X-ray diffraction analysis

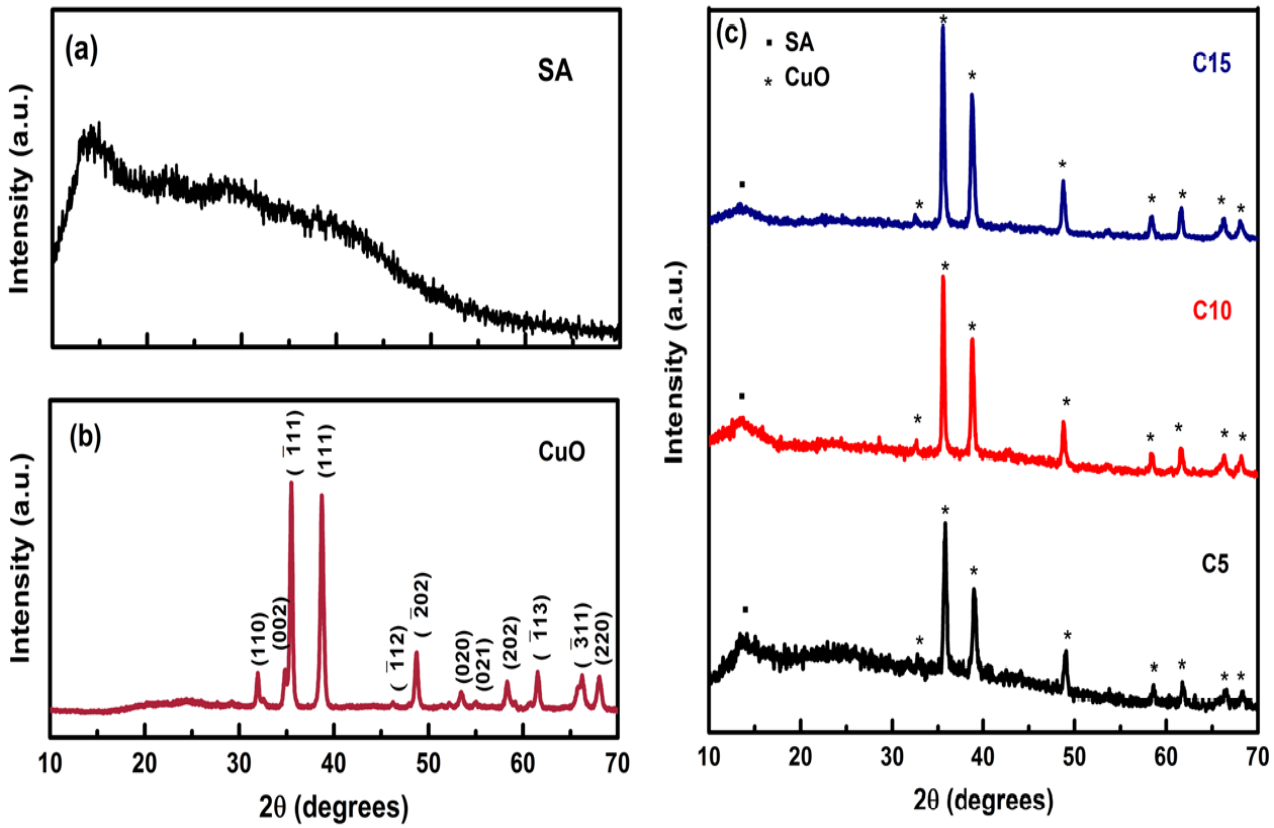

Fig. 1. XRD patterns of a) pure SA (C0), b) CuO nanoparticles, c) C5, C10, and C15.

The pure Sodium Alginate (C0), CuO nanoparticles, and their polymer nanocomposites were characterized by X-ray diffractions and shown in Fig. 1(a)-(c). The diffractogram of pure Sodium Alginate (Fig. 1a) shows a broad diffraction peak at 2θ=13.32° because of its amorphous nature [21, 22]. The XRD (Fig. 1b) of the pure CuO nanoparticles showed structurally monoclinic and all the diffraction peaks were matched

International Journal of Engineering Research & Technology (IJERT)
ISSN: 2278-0181
Vol. 10 Issue 01, January-2021

with JCPDS No. (89 - 2529). The values of d-spacing are evaluated according to Bragg's law i.e., $\lambda = 2d\sin\theta$, where λ is the X-ray wavelength, θ is the diffraction angle, d is the interplanar spacing. The crystalline sizes (Ls) are evaluated by using Scherrer's relation; $L = k\lambda/\beta\cos\theta$ [23], where k=0.94 is the constant, β is the full width half maximum (FWHM). The XRD pattern (Fig. 1c) of C5, C10, and C15 nanocomposites reflect the peaks of CuO and the peak corresponding to the pure SA. As the CuO increases in the polymer nanocomposites, the corresponding Sodium Alginate peak also sharpen. All the CuO nanoparticles were dispersed well in the Sodium Alginate matrix. A similar observations was made by Sambyal et al., in Barium Strontium Titanate, graphite in polyaniline blends. Suma et al., also determined same trend in polyvinya alcohol-$Ag_{0.5}Cu_{0.75}O$ composite films by solution casting method.

III.2. Surface morphology

SEM images of the nanocompositess were examined to assess the morphology and the dispersion of CuO nanoparticles in the SA matrix and corresponding images are shown in Fig. 2 (a-e).

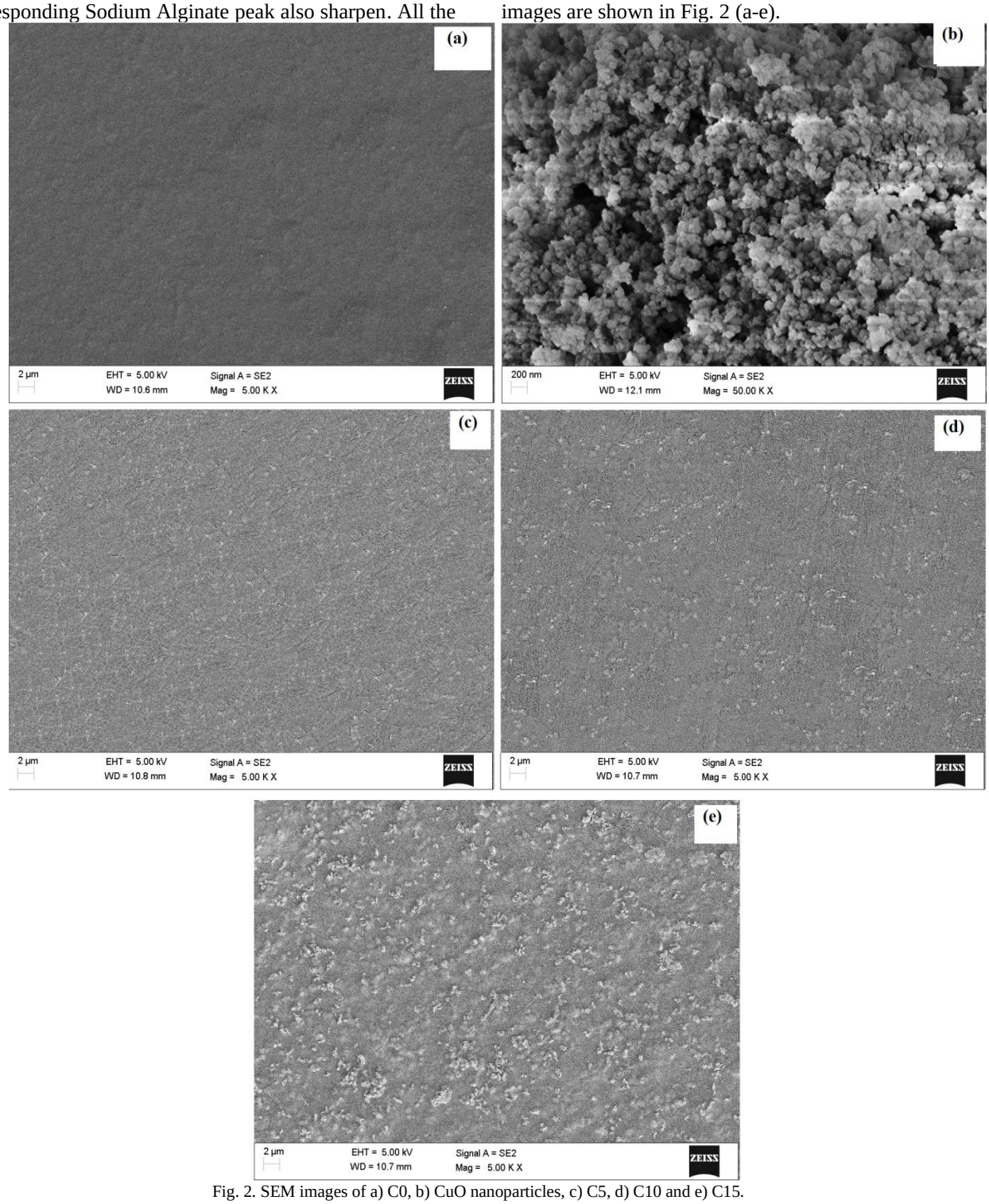

Fig. 2. SEM images of a) C0, b) CuO nanoparticles, c) C5, d) C10 and e) C15.

International Journal of Engineering Research & Technology (IJERT)
ISSN: 2278-0181
Vol. 10 Issue 01, January-2021

The pure SA has shown smooth surface morphology (Fig. 2a). The morphology of the pure CuO nanoparticles is shown in Fig. 2b. The morphology in the case of C5, C10 and C15 was differing with compare to the pure Sodium Alginate. The uniform morphology with roughness has been observed on the surface of SA-CuO nanocomposites with the doping of CuO. As the size of the dispersed particle becomes tinier and the dispersion of the particle is more homogenous then the uniform films of improved electrical properties have been developed [24]. In addition, as CuO content in the SA matrix increased, some aggregates are appearing at high content of the CuO and distributed uniformly on the surface of the matrix i.e., in the case of C15 (Fig.2e). Besides, the number of particles appearing on the surface with uniform distribution also enhanced with CuO content in the NCs (Fig.2(c-e)). This reveals the good compatability between polymer matrix and the CuO.

III.3. Thermogravimetric analysis (TGA)

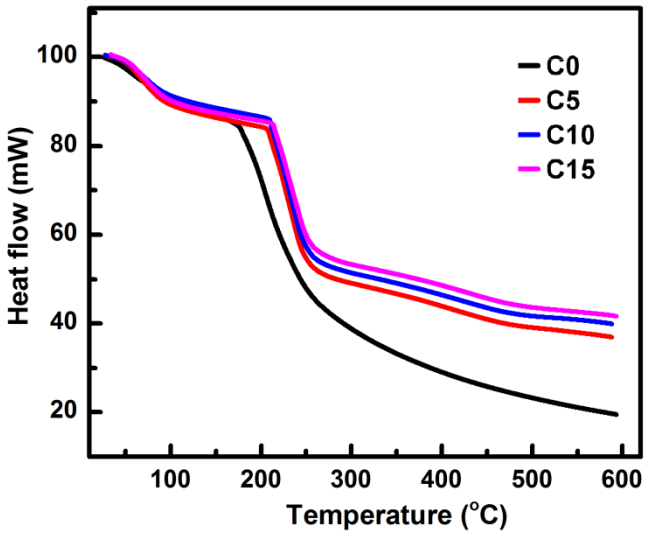

Fig. 3. TGA thermograms of C0, C5, C10, and C15.

To examine the thermal degradation of the synthesized polymer composite thin films, the thermograms were drawn and depicted in Fig.3 and the thermal degradation displayed in two steps. A total of 6% weight loss was observed from 30ºC – 55ºC, 8% weight loss from 55ºC – 150ºC, 55% weight loss from 150 ºC – 350 ºC in the pure SA film. The weight loss is considerably varied due to doping of CuO in the SA matrix. Initially 8% in the temperature range from 30 ºC – 90 ºC, due to the moisture retained in the films, which is absorbed from the atmosphere. Later 9% loss from 90ºC – 208ºC due to the decomposition of the polymer and 30% weight loss was noticed from 208ºC – 360ºC means that decomposition of the metal oxides starts after this temperature. Finally, 37%, 40% and 42% of the weight is retained in the sample for C5, C10 and C15 respectively. This attributed to the higher decomposition temperature of the nanocomposites leads to the excellent stability [6, 25]. These results are in coincidence with the DSC analysis. In addition, it was concluding that high thermal stability of the synthesized films is responsible for the various applications in high dielectric constant materials [26].

III.4. Dielectric measurements

To analyze the electrical properties of the polymer nanocomposites, the variation of dielectric constant (Ɛ'), dielectric loss (Ɛ"), and ac conductivity (σ_{ac}) as the function of temperature in the range room temperature to 100ºC for C0, C5, C10 and C15 were studied.

III.4.1. Variation of dielectric constant, dielectric loss with temperature

The Ɛ'-T plot at 100 Hz frequency of SA and doped SA nanocomposites with CuO nanoparticles were shown in Fig.4a. The Ɛ' increases in an exponential manner, attained maximum value at 90 ºC, and further decreases with an increase in temperature. This indicates the relaxation behavior of Ɛ'. The Ɛ' increases with CuO content in the nanocomposites. This indicates the mechanism of thermal activation takes place in the SA-CuO nanocomposites [27].The C15 is attained the higher values of Ɛ' at 100 Hz, at 90ºC. Fig.4b depicts Ɛ"-T plots of C0, C5, C10, and C15 at 100 kHz frequency. The Ɛ" exhibited a slow increasing pattern with temperature and attained a peak value at 90ºC. Further Ɛ" values are becoming low with the incorporation of CuO nanoparticles at higher temperatures. These types of relaxation are due to the accumulation of charge carriers at the polymer interfaces and undergo transition [28]. The highest value of the dielectric constant is at 90ºC and tabulated in the Table 3.

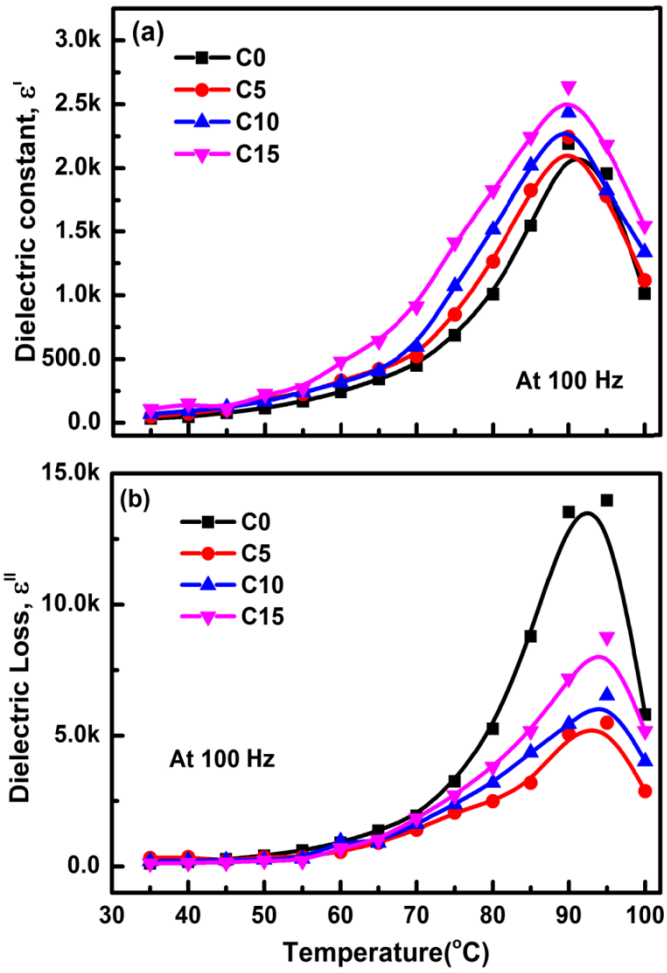

Fig.4. Variation of dielectric constant, dielectric loss with temperature of C0, C5, C10, and C15

International Journal of Engineering Research & Technology (IJERT)
ISSN: 2278-0181
Vol. 10 Issue 01, January-2021

III.4.2. Variation of ac conductivity with temperature

The Arrhenius equation which is assigned to the temperature dependent σ_{ac} given by [29]

$$\sigma_{ac} = \sigma_o \exp(-E_a/kT)$$

where E_a is the activation energy, k is the Boltzmann constant.The temperature dependant σ_{ac} values of SA-CuO nanocomposites are lower than the SA as shown in Fig. 5. Other than, this σ_{ac} increased with temperature, attains the maximum value at a particular temperature and decreases. This can be attributed to the hoping of charge carriers between the localized states that this arises due to the availability of free volume at higher temperatures. Hence, it leads to enhanced conductivity [13]. As nanoparticles increasing the distance between the particles become less there by it reduces the free volume and flexibility of the films [30, 31]. Thus, it results in lower σ_{ac} values of nanocomposites due to the presence of CuO nanoparticles. The high conductivity values was observed for all the synthesized nanocomposites at 90°C temperature and shown in the Table 3.

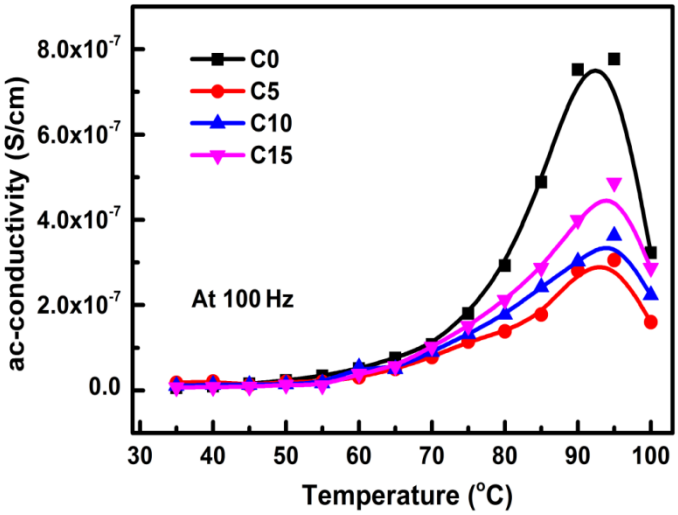

Fig.5. Variation of ac conductivity with the temperature of C0, C5, C10, and C15

Arrhenius plots were studied to investigate the activation energies of C0, C5, C10 and C15. The respective plots are shown in Fig. 6. The decreasing of activation energies of the SA-CuO nanocomposites observed with the addition of nano CuO in the SA and values are listed in Table3. A similar observation was reported by Baset et al., from the development of polyvinylchloride/Silica nanocomposite films with E_a values from 0.7-0.3 eV [32], and Ghamaz et al., reported that low values of E_a with doping of Methylene Blue dye in the PVA/PVP blend is due to hoping conduction mechanism for conductivity [33].

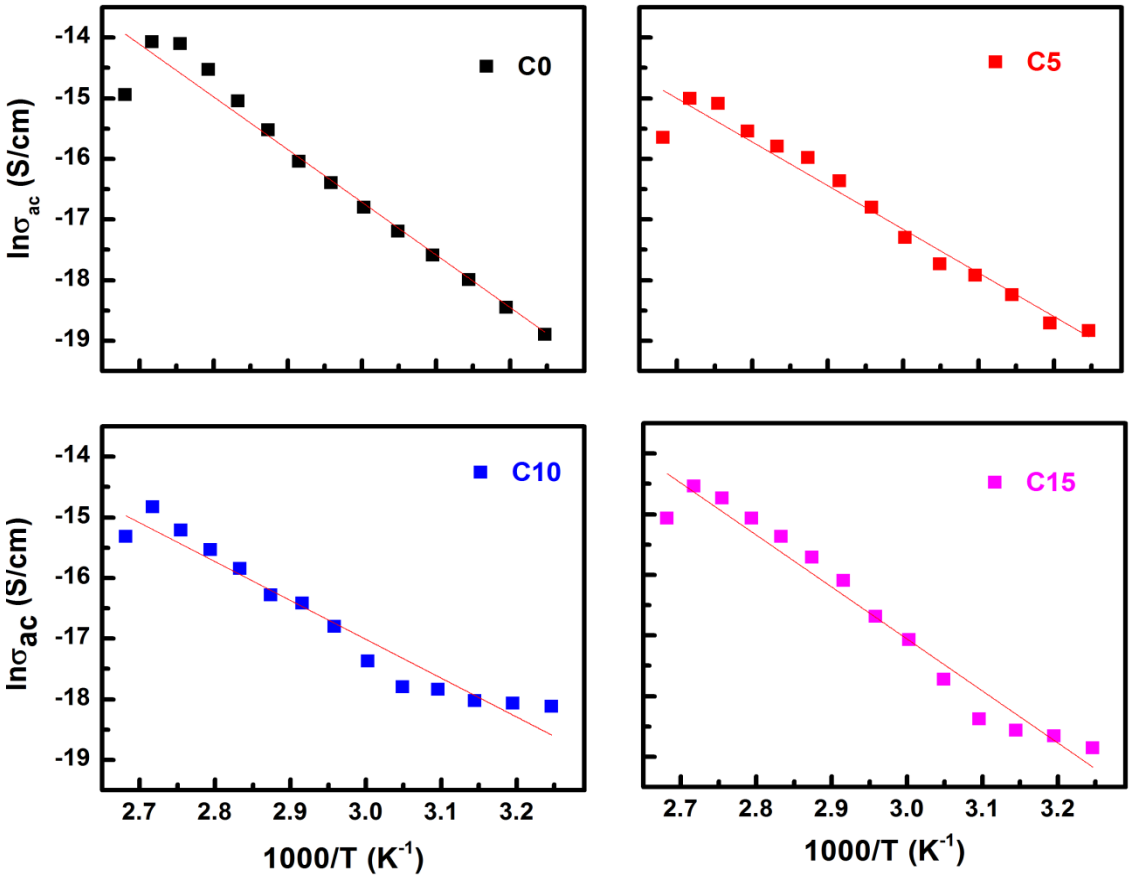

Fig.6. Arrhenius plots of C0, C5, C10, and C15

International Journal of Engineering Research & Technology (IJERT)
ISSN: 2278-0181
Vol. 10 Issue 01, January-2021

Table.1. Dielectric parameters of C0, C5, C10, C15

Dielectric Parameters	C0	C5	C10	C15
Ɛ' at 90ºC	2192	2243	2435	2640
σ_{ac} at 90ºC (S/cm)	$7.77x10^{-7}$	$3.05 x10^{-7}$	$3.63 x10^{-7}$	$4.87 x10^{-7}$
E_a (eV)	0.7473	0.6184	0.6504	0.7367

IV. CONCLUSIONS

The development of the dielectric polymer nanocomposite films based on organic polymer and inorganic metal oxides has attracted the attention of researchers due to its potential applications in electronic devices. The X-ray diffractograms of the pure CuO nanoparticles showed structurally monoclinic, and C5, C10, and C15 nanocomposites reflect the peaks of CuO and the peak corresponding to the pure SA. As the CuO increases in the polymer nanocomposites, the corresponding Sodium Alginate peak also sharpen. All the CuO nanoparticles were dispersed well in the Sodium Alginate matrix. The uniform morphology with roughness has been observed on the surface of SA-CuO nanocomposites with the doping of CuO. As the size of the dispersed particle becomes tinier and the dispersion of the particle is more homogenous then the uniform films of improved electrical properties have been developed. The Ɛ' increases in an exponential manner, attained maximum value at 90ºC, and further decreases with an increase in temperature. This indicates the relaxation behavior of Ɛ'. The Ɛ' increases with CuO content in the nanocomposites. This indicates the mechanism of thermal activation takes place in the SA-CuO nanocomposites.These types of relaxation are due to the accumulation of charge carriers at the polymer interfaces and undergo transition.

REFERENCES

[1] N.K. Abbas, M.A. Habeeb, A.J.K. Algidsawi, Preparation of Chloro Penta Amine Cobalt(III) Chloride and Study of Its Influence on the Structural and Some Optical Properties of Polyvinyl Acetate, International Journal of Polymer Science 2015 (2015) 926789.

[2] N. R, S. Kalyanasundaram, A. Gopalan, Y. Saito, A. Stephan, Preparation and characterization of PVC/PMMA blend polymer electrolytes complexed with LiN(C2F5SO2)2, Polímeros 14 (2004).

[3] Y. Li, Q. Xu, Q. Zhang, D. Chen, Facile Preparation and Enhanced Capacitance of the Polyaniline/Sodium Alginate Nanofiber Network for Supercapacitors, Langmuir : the ACS journal of surfaces and colloids 27 (2011) 6458-63.

[4] S.D. Praveena, V. Ravindrachary, R.F. Bhajantri, Ismayil, Free volume-related microstructural properties of lithium perchlorate/sodium alginate polymer composites, Polymer Composites 35(7) (2014) 1267-1274.

[5] D.P. Suhas, A.V. Raghu, H.M. Jeong, T.M. Aminabhavi, Graphene-loaded sodium alginate nanocomposite membranes with enhanced isopropanol dehydration performance via a pervaporation technique, RSC Advances 3(38) (2013) 17120-17130.

[6] M. Ionita, M.A. Pandele, H. Iovu, Sodium alginate/graphene oxide composite films with enhanced thermal and mechanical properties, Carbohydrate Polymers 94(1) (2013) 339-344.

[7] A. Sand, M. Yadav, K. Behari, Synthesis and characterization of alginate-g-vinyl sulfonic acid with a potassium peroxydiphosphate/thiourea system, Journal of Applied Polymer Science 118(6) (2010) 3685-3694.

[8] E. Zactiti, T. Kieckbusch, Potassium sorbate permeability in biodegradable alginate films: Effect of the antimicrobial agent concentration and crosslinking degree, Journal of Food Engineering 77(3) (2006) 462-467.

[9] M. Chintha, S.R. Obireddy, P. Areti, S. Marata Chinna Subbarao, C.R. Kashayi, J.K. Rapoli, Sodium alginate/locust bean gum-g-methacrylic acid IPN hydrogels for “simvastatin” drug delivery, Journal of Dispersion Science and Technology (2019) 1-11.

[10] D.M. Jundale, S.T. Navale, G.D. Khuspe, D.S. Dalavi, P.S. Patil, V.B. Patil, Polyaniline–CuO hybrid nanocomposites: synthesis, structural, morphological, optical and electrical transport studies, Journal of Materials Science: Materials in Electronics 24(9) (2013) 3526-3535.

[11] V.U. Siddiqui, I. Khan, A. Ansari, W.A. Siddiqui, M. Khursheed Akram, Structural and Morphological Analysis of Newly Synthesized CuO@Alginate Nanocomposite with Enriched Electrical Properties, in: B. Gupta, A.K. Ghosh, A. Suzuki, S. Rattan (Eds.) Advances in Polymer Sciences and Technology, Springer Singapore, Singapore, 2018, pp. 21-28.

[12] A. Shameem, P. Devendran, V. Siva, K.S. Venkatesh, A. Manikandan, S.A. Bahadur, N. Nallamuthu, Dielectric Investigation of NaLiS Nanoparticles Loaded on Alginate Polymer Matrix Synthesized by Single Pot Microwave Irradiation, Journal of Inorganic and Organometallic Polymers and Materials 28(3) (2018) 671-678.

[13] S. More, R. Dhokne, S. Moharil, Dielectric relaxation and electric modulus of polyvinyl alcohol–Zinc oxide composite films, Materials Research Express 4(5) (2017) 055302.

[14] B. Kumar, G. Kaur, P. Singh, S. Rai, Synthesis, structural, optical and electrical properties of metal nanoparticle–rare earth ion dispersed in polymer film, Applied Physics B 110(3) (2013) 345-351.

[15] N. Bouazizi, R. Bargougui, A. Oueslati, R. Benslama, Effect Of Synthesis Time On Structural, Optical And Electrical Properties Of CuO Nanoparticles Synthesized By Reflux Condensation Method, ADVANCED MATERIALS Letters 2015 (2014) 158-164.

[16] L. Zhang, W. Lu, Y. Feng, J. Ni, Y. Lü, X. Shang, Facile synthesis of leaf-like Cu (OH) 2 and its conversion into CuO with nanopores, Acta Physico-Chimica Sinica 24(12) (2008) 2257-2262.

[17] R. Sahay, P. Suresh Kumar, V. Aravindan, J. Sundaramurthy, W. Chui Ling, S.G. Mhaisalkar, S. Ramakrishna, S. Madhavi, High aspect ratio electrospun CuO nanofibers as anode material for lithium-ion batteries with superior cycleability, The Journal of Physical Chemistry C 116(34) (2012) 18087-18092.

[18] C. Vidyasagar, Y.A. Naik, T. Venkatesha, R. Viswanatha, Solid-state synthesis and effect of temperature on optical properties of CuO nanoparticles, Nano-Micro Letters 4(2) (2012) 73-77.

[19] S. Choudhary, R.J. Sengwa, Structural and dielectric studies of amorphous and semicrystalline polymers blend-based nanocomposite electrolytes, Journal of Applied Polymer Science 132(3) (2015).

[20] G.R. Suma, N.K. Subramani, S. Sachhidananda, S.V. Satyanarayana, Siddaramaiah, Optical and electrical evaluation of Ag0.5Cu0.75O introduced poly(vinyl alcohol) based E.Coli sensors, Journal of Materials Science: Materials in Electronics 28(17) (2017) 13139-13148.

[21] G.T. Padma, T.S. Rao, K.C.B. Naidu, Preparation, characterization and dielectric properties of sodium alginate/titanium dioxide composite membranes, SN Applied Sciences 1(1) (2018) 75.

[22] S. Bekin, S. Sarmad, K. Gürkan, G. Yenici, G. Keçeli, G. Gürdağ, Dielectric, thermal, and swelling properties of calcium ion-crosslinked sodium alginate film, Polymer Engineering & Science 54 (2014).

[23] S. Choudhary, R.J. Sengwa, Anomalous behavior of the dielectric and electrical properties of polymeric nanodielectric poly(vinyl alcohol)–titanium dioxide films, Journal of Applied Polymer Science 134(10) (2017).

[24] C. Bhatt, R. Swaroop, A. Arya, A. Sharma, Effect of nano-filler on the properties of polymer nanocomposite films of PEO/PAN complexed with NaPF6, J Mater Sci Eng B 5(11-12) (2015) 418-434.

[25] C.C. Yang, S.J. Chiu, K.T. Lee, W.C. Chien, C.T. Lin, C.A. Huang, Study of poly (vinyl alcohol)/titanium oxide composite polymer membranes and their application on alkaline direct alcohol fuel cell, Journal of Power Sources 184(1) (2008) 44-51.

[26] S.-H. Xie, B.-K. Zhu, Z.-K. Xu, Y.-Y. Xu, Preparation and properties of polyimide/LTNO composite films with high dielectric constant, Materials Letters 59(19-20) (2005) 2403-2407.

International Journal of Engineering Research & Technology (IJERT)
ISSN: 2278-0181
Vol. 10 Issue 01, January-2021

[27] R.J. Sengwa, S. Choudhary, Dielectric Dispersion and Relaxation in Polymer Blend Based Nanodielectric Film, Macromolecular Symposia 362(1) (2016) 132-138.
[28] E.M. Masoud, A.A. Elbellihi, W.A. Bayoumy, M. Mousa, Effect of LiAlO2 nano particle filler concentration on the electrical properties of PEO-LiClO4 composite, Materials Research Bulletin 48 (2013).
[29] S. El-Sayed, T. Abel-Baset, A. Abou Elfadl, A. Hassen, Effect of nanosilica on optical, electric modulus and AC conductivity of polyvinyl alcohol/polyaniline films, Physica B: Condensed Matter 464 (2015) 17-27.
[30] E. Correa, M.E. Moncada, V.H. Zapata, Electrical characterization of an ionic conductivity polymer electrolyte based on polycaprolactone and silver nitrate for medical applications, Materials Letters 205 (2017) 155-157.
[31] M.A. Ratner, D.F. Shriver, Ion transport in solvent-free polymers, Chemical Reviews 88(1) (1988) 109-124.
[32] T. Abdel-Baset, M. Elzayat, S. Mahrous, Characterization and Optical and Dielectric Properties of Polyvinyl Chloride/Silica Nanocomposites Films, International Journal of Polymer Science 2016 (2016) 1707018.
[33] N. El-Ghamaz, H. Zidan, A. Abdelghany, A. Lotfy, Structural and Electrical Properties of PVA/PVP Blend Doped with Methylene Blue Dye, Int. J. Electrochem. Sci. 11 (2016) 9041 – 9056.